Phosphatidylinositol-(4,5)-bisphosphate enables efficient secretion of HIV-1 Tat by infected T-cells

Fabienne Rayne, Solène Debaisieux, Hocine Yezid, Yea-Lih Lin, Clément Mettling, Karidia Konate, Nathalie Chazal, Stefan Arold, Martine Pugnière, Françoise Sanchez, et al.

The EMBO Journal (2010) 29, 1348–1362 | © 2010 European Molecular Biology Organization | All Rights Reserved 0261-4189/10
www.embojournal.org

THE EMBO JOURNAL

Phosphatidylinositol-(4,5)-bisphosphate enables efficient secretion of HIV-1 Tat by infected T-cells

Fabienne Rayne[1,7,8], Solène Debaisieux[1,8], Hocine Yezid[1], Yea-Lih Lin[2], Clément Mettling[2], Karidia Konate[3], Nathalie Chazal[1], Stefan T Arold[4], Martine Pugnière[1], Françoise Sanchez[1], Anne Bonhoure[1], Laurence Briant[1], Erwann Loret[5], Christian Roy[6] and Bruno Beaumelle[1,*]

[1]CPBS, UMR 5236 CNRS, Case 100, Université Montpellier 2, Montpellier, France, [2]IGH, UPR 1142 CNRS, 141 rue de la Cardonille, Montpellier, France, [3]CRBM, UMR 5237 CNRS, 1919 route de Mende, Montpellier, France, [4]CBS, INSERM U554-Université Montpellier I-UMR 5048 CNRS, 29 rue de Navacelles, Montpellier, France, [5]INSERM U911, Faculté de Pharmacie, 27, Bd Jean Moulin, Marseille, France and [6]DIMNP, UMR 5235 CNRS, Case 107, Université Montpellier 2, Montpellier, France

Human immunodeficiency virus type 1 (HIV-1) transcription relies on its transactivating Tat protein. Although devoid of a signal sequence, Tat is released by infected cells and secreted Tat can affect uninfected cells, thereby contributing to HIV-1 pathogenesis. The mechanism and the efficiency of Tat export remained to be documented. Here, we show that, in HIV-1-infected primary $CD4^+$ T-cells that are the main targets of the virus, Tat accumulates at the plasma membrane because of its specific binding to phosphatidylinositol-4,5-bisphosphate ($PI(4,5)P_2$). This interaction is driven by a specific motif of the Tat basic domain that recognizes a single $PI(4,5)P_2$ molecule and is stabilized by membrane insertion of Tat tryptophan side chain. This original recognition mechanism enables binding to membrane-embedded $PI(4,5)P_2$ only, but with an unusually high affinity that allows Tat to perturb the $PI(4,5)P_2$-mediated recruitment of cellular proteins. Tat–$PI(4,5)P_2$ interaction is strictly required for Tat secretion, a process that is very efficient, as ~2/3 of Tat are exported by HIV-1-infected cells during their lifespan. The function of extracellular Tat in HIV-1 infection might thus be more significant than earlier thought.

The EMBO Journal (2010) **29,** 1348–1362. doi:10.1038/emboj.2010.32; Published online 11 March 2010
Subject Categories: membranes & transport; microbiology & pathogens
Keywords: HIV-1; PIP_2; Tat; toxin; unconventional secretion

*Corresponding author. UMR 5236 CNRS, Case 100, Université Montpellier II, Montpellier, Cedex 05 34095, France.
Tel.: 33 467 143 398; Fax: +33 467 143 338;
E-mail: bruno.beaumelle@univ-montp2.fr
[7]Present address: Université Paul Sabatier, 118, Route de Narbonne, 31062 Toulouse Cedex 9, France
[8]These authors contributed equally to this work

Received: 29 December 2009; accepted: 17 February 2010; published online: 11 March 2010

Introduction

Some cell proteins, generally small ones (<40 kDa), are secreted despite their lack of signal sequence. These proteins include homeodomain transcription factors, as well as numerous cytokines, including FGF-1, FGF-2 and IL-1β (Nickel and Rabouille, 2009). Their secretion pathways are collectively designed as nonclassical or unconventional export routes (Dupont *et al*, 2007; Nickel and Rabouille, 2009). These processes are intriguingly diverse and, so far, there seems to be as many pathways as proteins. Although the overall secretion route has been identified for most proteins that are secreted in an unconventional manner, mechanistic details on these pathways are lacking (Keller *et al*, 2008; Nickel and Rabouille, 2009).

The human immunodeficiency virus type 1 (HIV-1) transactivating protein Tat is a small (~11 kDa) and basic protein that binds to the transactivation-response element (TAR) on nascent RNA and recruits cyclin T1, a component of the transcription elongation factor P-TEFb. As Tat promotes efficient transcription from the 5′ long-terminal repeat (LTR) of HIV-1, it has, therefore, a crucial function in virus multiplication within infected T-cells (Jeang *et al*, 1999). In agreement with this transcriptional function, Tat was found to accumulate within the nucleus or nucleolus of HIV-1-infected (Ranki *et al*, 1994) or Tat-transfected (Marasco *et al*, 1994) T-cell lines.

Although Tat is devoid of signal sequence, it is secreted by infected cells using an unconventional secretion pathway and in the absence of cell lysis (Ensoli *et al*, 1990). The fact that nanomolar Tat concentrations are present in the sera of HIV-1-infected patients (Xiao *et al*, 2000) indicates that this secretion process should be efficient and there is increasing evidence that circulating Tat is implicated in viral multiplication, AIDS development and HIV-1-associated dementia. Strikingly, secreted Tat acts as a viral toxin, inducing deleterious effects on numerous cell types. For instance, extracellular Tat can deregulate cytokine secretion by monocytes and lymphocytes, and directly induce lymphocyte and neuron death (Rubartelli *et al*, 1998; Gallo, 1999; Huigen *et al*, 2004). Nevertheless, both the efficiency and the mechanism of Tat secretion remain to be elucidated.

Phosphatidylinositol-4,5-bisphosphate ($PI(4,5)P_2$) is a phospholipid that is specifically concentrated within the inner leaflet of the plasma membrane to which it can recruit proteins involved in several important cell activities such as endocytosis, phagocytosis, exocytosis and cell adhesion (De Matteis and Godi, 2004; Di Paolo and De Camilli, 2006). Here, we showed that Tat concentrates at the plasma membrane in primary T-cells. We identified $PI(4,5)P_2$ as the cell component responsible for Tat recruitment at this level, and found that Tat–$PI(4,5)P_2$ interaction enables Tat secretion. Intriguingly, Tat only binds $PI(4,5)P_2$ when present in a membrane. This is due to the concomitant membrane insertion of Tat single Trp that is required to stabilize Tat–$PI(4,5)P_2$ interaction. This binding is

actually so tight that Tat can displace cell proteins from PI(4,5)P_2. We also found that secreted Tat strongly affects HIV-1 multiplication in CD4$^+$ primary T-cells.

Results

A cellular ELISA assay to monitor Tat secretion by T-cells

A first aim of this study was to set up a quantitative Tat secretion assay. A problem for Tat detection is the poor affinity of most anti-Tat antibodies. We tested 11 of them and found a couple that enabled reliable Tat detection by sandwich ELISA. Another problem was Tat susceptibility to oxidation. We observed that secreted Tat is readily oxidized by air oxygen and this makes it unreactive to antibodies (data not shown). To circumvent this difficulty, we modified a standard ELISA procedure. Jurkat cells, which are CD4$^+$ T-lymphocytes similar to most HIV-1-infected cells (Stebbing *et al*, 2004), were first transiently transfected by plasmids coding for Tat and luciferase (used as a control for cell lysis) before plating onto 96-well plates earlier coated with anti-Tat monoclonal antibodies. Cells were then incubated for various times in degassed medium containing a low concentration of reductant (20 μM 2-mercaptoethanol) before assaying plate-bound Tat by ELISA. This 'cellular ELISA' procedure enabled antibodies to capture secreted Tat before it becomes oxidized. Under these conditions, Tat secretion was linear up to 6 h. After this time, up to 30% of cellular Tat had been secreted by Jurkat cells (Figure 1A), whereas no release of cotransfected luciferase was observed. Hence, ~5% of cellular Tat is secreted hourly by transfected Jurkat cells.

Tat secretion by HIV-1-infected cells is an efficient process

We then examined the efficiency of Tat secretion in a biologically relevant system. We purified primary CD4$^+$ T-cells, infected them with HIV-1 and assayed Tat secretion 3 days later, i.e. shortly after the beginning of infection to minimize cell lysis. Less than 10% of the cells were infected after this time, and we had to leave cells 12–18 h in the plate to capture enough Tat to allow reliable quantitation. After 15 h, ~55% of total Tat (cells + medium) was found in the medium (Figure 1B) and extracellular concentration reached ~0.25 nM. It should be noted that, because Tat capture by antibodies takes place under native conditions, the cellular ELISA assay only detects free Tat in the medium and not any Tat that could be incorporated into virions. Infected cells secrete Tat almost as efficiently as the viral capsid protein p24, whereas Nef was not significantly exported (Figure 1B). According to the average half-life of 2.2 days for an infected primary CD4$^+$ T-cell (Perelson *et al*, 1996), that secretes 3.7 ± 0.2% of cellular Tat hourly, it can be calculated that 2/3 of Tat is exported (i.e. 195% of the intracellular amount).

Tat is membrane bound in HIV-1-infected T-cells

In the search for membrane compartments involved in Tat export, we examined Tat localization in CD4$^+$ T-cells. We first used Tat-transfected cells. In agreement with earlier studies performed on cell lines (Stauber and Pavlakis, 1998; Marcello *et al*, 2001), in stably transfected Jurkat Tat-III cells (Figure 2A) or conventional Jurkat cells transiently transfected by Tat (Figure 2B), Tat concentrated within the nucleus

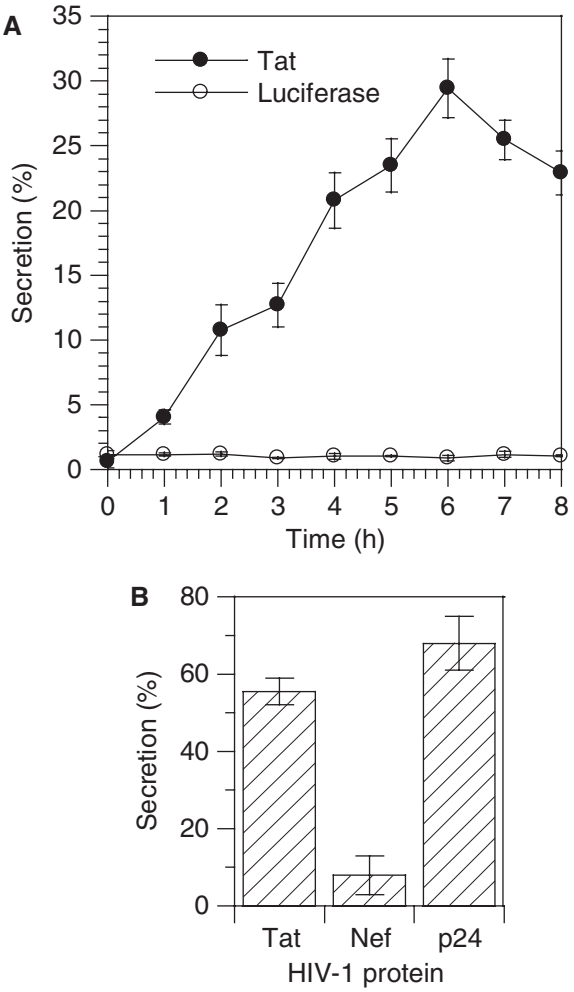

Figure 1 Tat secretion is an efficient process. (**A**) Time dependence of Tat secretion by transfected Jurkat cells. Cells were transfected with Tat and luciferase expression vectors. After 48 h, they were plated onto ELISA plates precoated with anti-Tat monoclonal antibody. Secretion was allowed for the indicated time and was calculated as medium/(cell + medium) (%) for both Tat and luciferase. (**B**) Secretion of Tat, Gag p24 and Nef by HIV-1-infected primary CD4$^+$ T-cells. Primary CD4$^+$ T-cells were isolated, stimulated and infected with HIV-1. Three days after, cells were plated onto anti-Tat-coated ELISA plates for 15 h. Tat binding takes place under native conditions and this assay only detects free Tat in the medium, whereas the ELISA used to assay extracellular p24 and Nef involves the use of a detergent that releases any virion-incorporated protein.

and nucleoli. Nevertheless, in Tat-transfected primary CD4$^+$ T-cells, Tat localized at the plasma membrane (Figure 2C). On HIV-1 infection, Tat concentrated at the plasma membrane of primary CD4$^+$ T-cells (Figure 2D and E) together with Gag (p24). In some cells, especially at late stages of infection, Tat was also observed in the cytosol (Figure 2E; Supplementary Figure S1). The same localization was obtained using either a polyclonal or a monoclonal anti-Tat antibody, and controls were performed using antibodies against the nucleolar antigen Ki67 or histone H1 to check for the proper permeabilization of the nuclear envelope during immunofluorescence labelling of primary cells (Figure 2C–E; Supplementary Figure S1).

As it was surprising to find a transcription factor such as Tat concentrated at the plasma membrane, we tried to

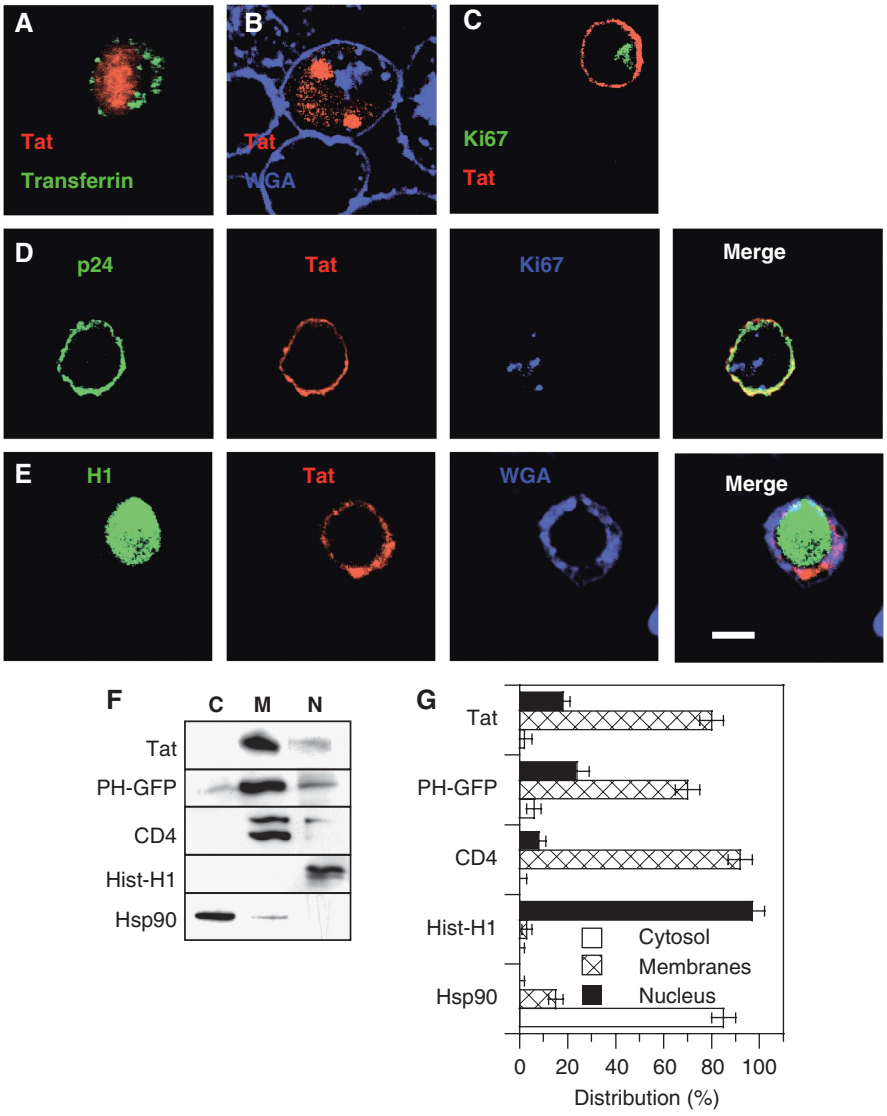

Figure 2 Tat is membrane bound in HIV-1-infected primary CD4$^+$ T-cells. (**A**–**E**) Immunofluorescence. Cells were fixed with paraformaldehyde and permeabilized with saponin. Tat, Gag p24, histone H1 or Ki67 were then revealed by immunofluorescence, as indicated. A fluorescent lectin (WGA) was used to localize the plasma membrane and the *trans*-Golgi network (TGN). (**A**) Jurkat-TatIII cells, which are stable Tat-transfected cells, were labelled with 100 nM fluorescent transferrin for 40 min to localize endosomes before fixation. (**B**) Jurkat cells were transiently transfected by Tat. (**C**) Tat-transfected-activated primary CD4$^+$ T-cells. (**D**, **E**) HIV-1-infected primary CD4$^+$ T-cells. Images are representative medial representative confocal sections. Bar, 5 μm. Wide field views are shown in Supplementary Figure S1. (**F**, **G**) Cell fractionation. Primary CD4$^+$ T-cells were transfected with Tat or $PH_{PLC\delta}$-EGFP. One day later, cells were fractionated in three fractions, cytosolic (C), membranes (M) and nucleus (N). Proteins were precipitated and separated by tricine SDS–PAGE before western blots that were revealed using antibodies against the indicated proteins (**F**). An anti-GFP was used to detect $PH_{PLC\delta}$-EGFP. (**G**) The experiment was repeated three times and films were scanned for band quantification. The results are mean ± s.e.m. ($n = 3$).

confirm this result using cell fractionation. Primary CD4$^+$ T-cells were thus transfected with Tat before cell fractionation in three different fractions containing cytosolic, membrane-associated and nuclear proteins. The efficiency of the fractionation procedure was examined using markers such as the cytosolic chaperone Hsp90 that was primarily observed in the cytosolic fraction, and histone H1 that was only found in the nuclear fraction (Figure 2F and G). The integral membrane protein CD4 mainly localized to the membrane fraction. For reasons that will become clearer later, a transfected EGFP chimera of PH domain of PLC$_\delta$ ($PH_{PLC\delta}$), a well characterized specific probe for PI(4,5)P_2 (De Matteis and Godi, 2004), was used as a marker for peripheral membrane proteins. This construct concentrated into the membrane fraction (80%), although it was present to some extent (24%) in the nuclear fraction. This distribution is consistent with PI(4,5)P_2 intracellular localization (Watt *et al*, 2002). Tat was essentially observed (80%) in the membrane fraction, although 18% were present in the nucleus (Figure 2F and G). Altogether with immunofluorescence data, these results showed that Tat is concentrated at the plasma membrane in primary CD4$^+$ T-cells and strongly suggested that Tat secretion could directly take place at this level.

Tat could be significantly detected in the nucleus by cell fractionation only, indicating that Tat concentration at this level is below the detection threshold of immunofluorescence, and that the nucleus is not a major destination for Tat in primary CD4$^+$ T-cells. The fact that the virus replicates

shows Tat accumulation within the nucleus is not required for efficient transactivation. To examine this point more directly using the same cellular background, we hooked the nuclear export signal (NES) of Rev to Tat C-terminus. As shown earlier in HeLa cells (Stauber and Pavlakis, 1998; Sivakumaran *et al*, 2009), the resulting Tat-NES was excluded from the nucleus of transiently transfected Jurkat cells and was exclusively observed in the cytosol or at the plasma membrane (Supplementary Figure S2A). We then compared the efficiency of transactivation by Tat-NES with that of native Tat using a dose-response curve. The efficiency of transactivation by Tat-NES was ~70% of that of native Tat and this ratio remained constant whatever the plasmid doses, even for low Tat/LTR ratios (Supplementary Figure S2B). This result confirmed that efficient transactivation by Tat does not require Tat nuclear/nucleolar accumulation. This is consistent with the very high affinity of the cyclin T1–Tat–TAR ternary complex that assembles with subnanomolar K_d values (Zhang *et al*, 2000). We will come back to this point in the Discussion section.

Tat binds liposomal PI(4,5)P_2 with a high affinity and specificity

The next question was thus how Tat was recruited at the plasmalemma. We noticed that Tat had a putative-binding site for PI(4,5)P_2 in its basic domain (49-RKKRRQRRR-57). We first examined whether Tat actually bound PI(4,5)P_2 using a conventional liposome sedimentation assay (Barret *et al*, 2000). Tat was quantitatively pelleted with liposomes as soon as they contained 2.5% PI(4,5)P_2 (Figure 3A), which is the approximate concentration of PI(4,5)P_2 in the inner leaflet of the plasma membrane (Lemmon, 2003). If PI(4,5)P_2 was involved in Tat recruitment at the plasma membrane, Tat should specifically bind to this phosphoinositide. We thus examined the specificity of Tat binding to different phosphoinositides. Tat bound, with roughly the same efficiency,

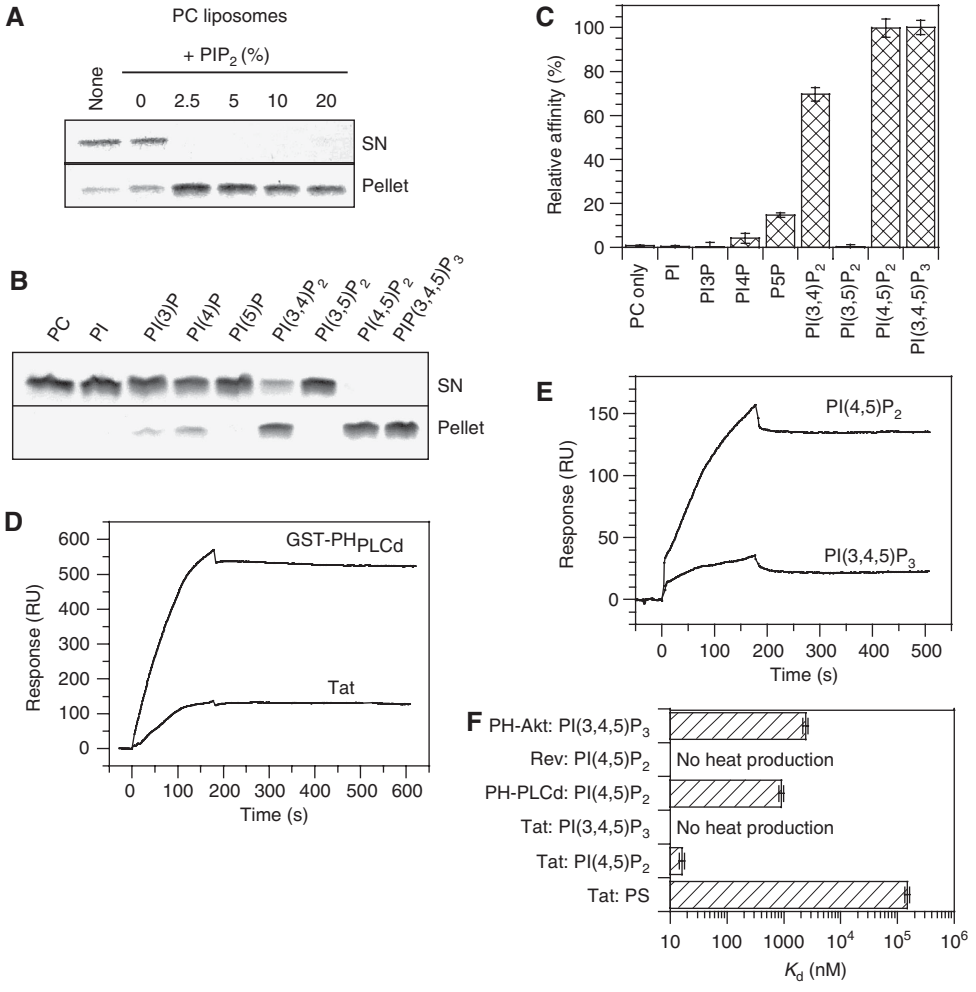

Figure 3 Tat binds with high affinity to lipsomes containing PI(4,5)P_2. (**A**) Effect of PI(4,5)P_2 concentration on Tat binding to liposomes. Multilamellar PC liposomes were incubated with Tat before ultracentrifugation. The pellet and supernatant (SN) were analysed by SDS–PAGE, and gels were stained with Coomassie blue. (**B**) Specificity of Tat binding to phosphoinositides. Liposomes included 2.5% (mol/mol) of the indicated phosphoinositide. (**C**) Specificity of phosphoinositide recognition by Tat deduced from liposome sedimentation assays. The results are mean ± s.e.m. ($n = 3$). (**D**) SPR sensorgrams of Tat (200 nM) and GST–$PH_{PLC\delta}$ (200 nM) binding to immobilized liposomes containing PC (75%), PE (20%) and PI(4,5)P_2 (5%). (**E**) SPR sensorgrams showing the binding of Tat (200 nM) to liposomes containing 5% of either PI(4,5)P_2 or PI(3,4,5)P_3. (**F**) Affinities for PS, PI(4,5)P_2 or PI(3,4,5)P_3 of different phosphoinositide-binding proteins used in this study. K_d were determined using ITC. No heat production was detectable when mixing PI(3,4,5)P_3 liposomes with Tat indicating that, according to ITC, Tat does not bind PI(3,4,5)P_3.

to PI(4,5)P_2 and PI(3,4,5)P_3, to a lesser extent to PI(3,4)P_2, and did not show any significant affinity to any other phosphoinositide (Figure 3B and C).

It was also important to check whether Tat bound phosphatidylserine (PS), which is a negatively charged phospholipid present at high concentration (~18%) within the inner leaflet of the plasma membrane (Corbin *et al*, 2004). We found that Tat quantitatively sedimented with PS-containing liposomes only when the PS concentration reached 20% (Supplementary Figure S3). Hence, Tat interacted with PS in this sedimentation assay.

To identify among PS, PI(4,5)P_2 and PI(3,4,5)P_3 the phospholipid(s) that was or were most likely to be responsible for Tat recruitment to the plasma membrane, we measured the K_d of their interaction with Tat. To this end, we first immobilized small unilamellar vesicles on chips for surface plasmon resonance (SPR) experiments (Honing *et al*, 2005). Tat strongly bound to chips coated with vesicles containing 5% PI(4,5)P_2 (Figure 3D and E) and this binding was inhibited when anti-PI(4,5)P_2 antibodies were applied before Tat (not shown). Regarding affinity, Tat dissociated very weakly from immobilized PI(4,5)P_2 liposomes (Figure 3D and E), with a dissociation rate close to the sensitivity limit of the biosensor apparatus, and the K_d we obtained (K_d <0.3 nM) was overestimated.

To validate these findings, we used a GST-tagged version of the PH domain of PLC$_\delta$ ($PH_{PLC\delta}$) that specifically recognizes PI(4,5)P_2 (De Matteis and Godi, 2004). Immobilized PI(4,5)P_2 liposomes bound GST–$PH_{PLC\delta}$ with a K_d of 4 nM (Figure 3D). This value is very close to that (6.6 nM) obtained before using the same experimental system (Zimmermann *et al*, 2002). It should be noted that in these SPR experiments, Tat (~11 kDa) always gave a smaller signal (140–160 RU) compared with GST–$PH_{PLC\delta}$ (~44 kDa) that gave ~550 RU (Figure 3D). This is likely due to the difference in size between the two proteins. Indeed, the ratio of protein masses (4) is essentially the same as the RU ratio (3.7). We then checked Tat specificity for phosphoinositides in this experimental system. When PI(4,5)P_2 was replaced by PI or PI4P, Tat did not bind anymore (Supplementary Figure S4). These results thus confirmed the specificity of Tat binding deduced from centrifugation assays (Figure 3B and C). SPR experiments also showed that Tat had at least a 10-fold higher affinity for PI(4,5)P_2 as compared with PI(3,4,5)P_3 (Figure 3E). The apparent discrepancy between these results and the equivalent binding of Tat to these lipids observed when using the cosedimentation assay (Figure 3B and C) is due to the fact that the latter assay is not very quantitative and does not discriminate between ligands unless they display dramatically different affinities (Blin *et al*, 2008).

SPR data were confirmed by isothermal tritration calorimetry (ITC), a technique that is quantitative and enables reliable measurements of affinities over a wide-concentration range (nM to μM). ITC results showed that Tat bound PI(4,5)P_2 liposomes with a high affinity (K_d ~ 16 nM; 1 PI(4,5)P_2/Tat), whereas Tat poorly recognized PS (K_d >100 μM; 3 PS/Tat) and did not bind to PI(3,4,5)P_3 in this system (Figure 3F). Altogether, SPR and ITC data showed that Tat is a specific PI(4,5)P_2 ligand that displays a very high affinity for this lipid. Indeed, Tat avidity for PI(4,5)P_2 (0.3 nM for SPR and 16 nM for ITC) is 20- to 50-fold higher than that of $PH_{PLC\delta}$ (6.6 nM for SPR and 900 nM for ITC). As a negative control, we also used HIV-1 Rev that owns a basic domain (Truant and Cullen, 1999). Nevertheless, this does not endow Rev with PI(4,5)P_2-binding properties (Figure 3F).

Tat is a strong and specific PI(4,5)P_2 ligand intracellularly

As a number of proteins containing basic motifs were found to bind both PI(4,5)P_2 and PI(3,4,5)P_3 (Heo *et al*, 2006), it was important to check whether Tat was a specific PI(4,5)P_2 ligand intracellularly. It was also interesting to examine whether the superior affinity of Tat for PI(4,5)P_2 compared with $PH_{PLC\delta}$ was not only observed using SPR or ITC, but also on living cells. To examine these issues, we used $PH_{PLC\delta}$ and PH_{Akt} domains that are specific ligands of PI(4,5)P_2 and PI(3,4,5)P_3, respectively (Varnai and Balla, 1998; Astoul *et al*, 2001). When measured by ITC, we found the K_d of both interactions to be 0.9 μM for GST–$PH_{PLC\delta}$/PI(4,5)P_2 interaction and 2.4 μM for GST–PH_{Akt}/PI(3,4,5)P_3 (Figure 3F), consistent with published data (Lemmon *et al*, 1995; Stephens *et al*, 1998). As these values lie within the same range, the ability of Tat to compete with these PH domains for their favourite phosphoinositide will, therefore, directly reflect Tat affinity for this lipid in the cellular context. For these competition experiments, we used Jurkat cells, as they lack phosphatases PTEN and SHIP that degrade PI(3,4,5)P_3 into PI(4,5)P_2 and PI(3,4)P_2, respectively. These cells thus have a high basal level of PI(3,4,5)P_3 (Astoul *et al*, 2001) and specific ligands for this lipid such as PH_{Akt} domain (Astoul *et al*, 2001) and Gab1 (Maroun *et al*, 2003), therefore, localize at their plasma membrane (Figure 4A). Transfected Tat was able to displace an $PH_{PLC\delta}$-EGFP probe, but neither PH_{Akt}-EGFP nor Gab1-EGFP from the membrane (Figure 4A). To have a more precise idea of the efficiency of $PH_{PLC\delta}$-EGFP displacement, we performed image quantification on $n>30$ cells. The results showed that, in control cells, 15% of $PH_{PLC\delta}$-EGFP is cytosolic. This fraction rose to 40% when Tat was cotransfected (Figure 4B). As a positive control for displacement of the $PH_{PLC\delta}$ probe, we used neomycin. This cationic antibiotic binds tightly to the headgroup of phosphoinositides, thereby inhibiting protein binding to PI(4,5)P_2 (Aharonovitz *et al*, 2000). In neomycin treated cells, 39% of $PH_{PLC\delta}$-EGFP was cytosolic, just as observed on Tat cotransfection (Figure 4B). Hence, Tat is able to efficiently displace $PH_{PLC\delta}$-EGFP from PI(4,5)P_2. As a positive control for the displacement of PI(3,4,5)P_3 probes to the cytosol, we cotransfected cells with PTEN that induced quantitative relocalization of both PI(3,4,5)P_3 probes to the cytosol, whereas $PH_{PLC\delta}$-EGFP remained at the plasma membrane, as expected. The inactive (G129E) PTEN mutant had no effect (Figure 4A). Collectively, these data confirmed biochemical data (Figure 3F) and showed that Tat is a PI(4,5)P_2 selective ligand that does not significantly interact with PI(3,4,5)P_3 intracellularly. They also corroborated biochemical results indicating that Tat has a higher affinity for PI(4,5)P_2 compared with $PH_{PLC\delta}$ and indicated that, despite the fact that Tat is not easily visualized at the plasma membrane of Jurkat cells, it is nevertheless recruited at this level in a PI(4,5)P_2-dependent manner. The efficiency of Tat nuclear import is such that it apparently perturbs the stability of Tat–PIP_2 interaction, thereby decreasing Tat residence time at the plasma membrane. Nuclear accumulation, therefore, likely

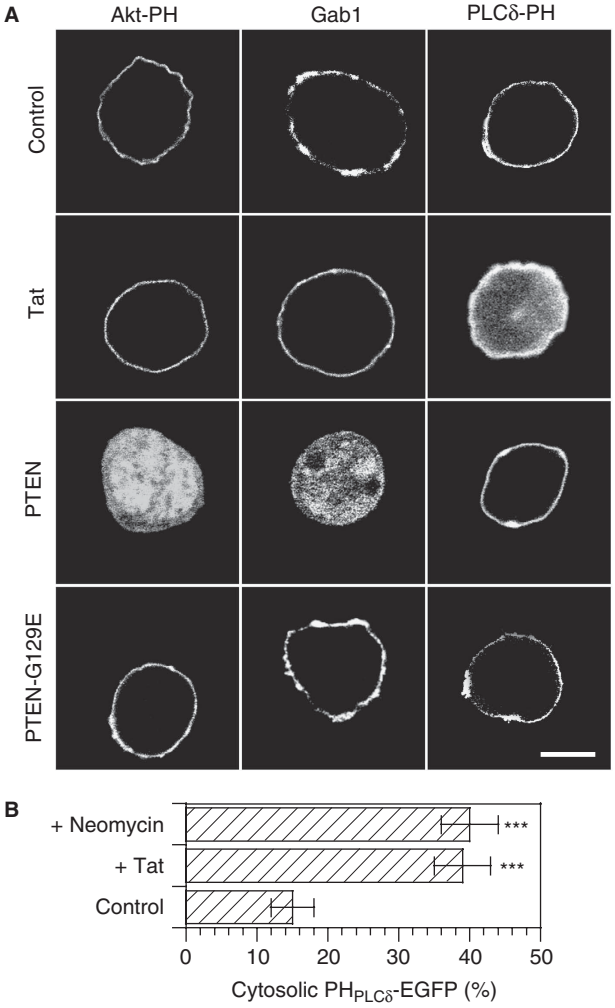

Figure 4 Tat is a high-affinity PI(4,5)P_2 ligand intracellularly. (**A**) Tat selectively displaces PH$_{PLC\delta}$-EGFP from the plasma membrane. Jurkat cells were transfected as indicated using vectors coding for GAB1-EGFP or PH$_{Akt}$-EGFP that both bind PI(3,4,5)P_3, or of PH$_{PLC\delta}$-EGFP that is specific to PI(4,5)P_2, together with an equivalent amount of PTEN plasmid (WT that transforms PI(3,4,5)P_3 into PI(4,5)P_2, or inactive mutant), Tat vector or empty plasmid (control). Cells were grown for 24 h, then fixed for confocal microscopic examination. Bar, 5 μm. (**B**) Quantification of the efficiency of PH$_{PLC\delta}$-EGFP displacement to the cytosol. Images from $n>30$ cells were recorded and the percentage of cell-fluorescence signal originating from the cytosol was determined. Control cells were transfected with PH$_{PLC\delta}$-EGFP and empty vector, cells + Tat were cotransfected with PH$_{PLC\delta}$-EGFP and Tat (ratio 1:1), cells + neomycin were treated with 2 mM neomycin for 1 h at 37°C before fixation. The significance of differences with control conditions was assessed using an unpaired, two-sided Student's *t*-test (***$P<0.001$).

explains why it is difficult to visualize Tat at the plasmalemma in Jurkat cells.

PI(4,5)P_2 is required for Tat targeting to the plasma membrane and for Tat secretion

To assess the function of this Tat–PI(4,5)P_2 interaction in Tat secretion, we first used neomycin that masks PI(4,5)P_2. This drug displaced Tat from the membrane of transfected primary CD4$^+$ T-cells (Figure 5A and B), and strongly inhibited Tat secretion by Jurkat cells (−60%, Figure 5C). Cell transfection with a phosphoinositide 5-phosphatase IV (5-pase IV) that hydrolyses PI(4,5)P_2 (Ono *et al*, 2004) strongly displaced Tat towards the cytosol (Figure 5A and B) and concomitantly inhibited Tat secretion by 65% (Figure 5C). Conversely, the 5-pase IV Δ1 inactive mutant affected neither Tat localization nor secretion (Figure 5A–C). The Ipn54 yeast 5-phosphatase (Pendaries *et al*, 2006) partly displaced Tat to the cytosol (Figure 5A and B) and inhibited Tat secretion by 40% (Figure 5C). A similar level of inhibition was achieved by the IpgD bacterial 4-phosphatase (Pendaries *et al*, 2006), whereas the IpgD C438S inactive mutant had no effect on Tat secretion by Jurkat cells (Figure 5C). A permanently activated mutant of Arf6 (Arf6-Q67L) that induces the formation of PI(4,5)P_2-positive actin-coated endosomes that are no longer able to recycle back to the plasma membrane (Brown *et al*, 2001) reduced Tat secretion by 40% (Figure 5C). Both Arf6-Q67L and IpgD were toxic when expressed in primary T-cells. We also found that PH$_{PLC\delta}$, even when overexpressed, does not inhibit Tat secretion (Figure 5C), confirming that Tat is an intriguingly strong PI(4,5)P_2 ligand. Altogether, the use of these various PI(4,5)P_2 effectors that either masked, hydrolysed or displaced this lipid confirmed that Tat is bound to PI(4,5)P_2 intracellularly. They further indicated that this binding is responsible for Tat recruitment to the plasma membrane that is a prerequisite for Tat secretion by Jurkat cells.

It was important to check whether this was also the case in a biologically relevant system. Treatment of HIV-1-infected primary CD4$^+$ T-cells for 1 h with 2 mM neomycin resulted in quantitative displacement of Tat and Gag (p24) towards peri-Golgi compartments, that is around the main wheat germ agglutinin (WGA)-positive structure (Figure 5D). Neomycin toxicity limited the drug concentration that could be used during the overnight incubation required to assay Tat secretion by infected cells. Nevertheless, we found that Tat secretion by infected primary CD4$^+$ T-cells was inhibited in a dose-dependent manner by neomycin (Figure 5E), confirming that Tat secretion by HIV-1-infected cells relies on PI(4,5)P_2 binding.

Tat binds PIP$_2$ using a specific motif of its basic domain

We then examined whether the Tat basic domain was indeed responsible for PI(4,5)P_2 binding. To this end, we first used SPR and overlapping 20 mer peptides covering the Tat sequence (Figure 6A). Each peptide was injected twice to achieve saturation of binding sites as much as possible, before applying Tat to assess whether Tat fixation was affected by the peptide. Peptide 5 (residues 42–61), which covers the entire basic domain (residues 49–57) efficiently bound to PI(4,5)P_2 albeit, contrary to Tat, it readily dissociated (Figure 6B). It should be noted, therefore, that the Tat basic domain, also known as the 'protein transduction domain', that is used for protein vectorization into cells (Joliot and Prochiantz, 2004) is a weak PI(4,5)P_2 ligand (K_d ~600 nM for peptide 5 according to SPR). Peptide 5 nevertheless prevented Tat binding, whereas peptide 6 (residues 52–71), although encompassing most of the basic domain and containing five of its eight basic residues, did not bind PI(4,5)P_2 and, therefore, did not prevent Tat binding (Figure 6B). The remaining peptides behaved as peptide 6 (not shown). SPR data, therefore, indicated that Tat binding to PI(4,5)P_2 is mediated by its basic domain, and that at least

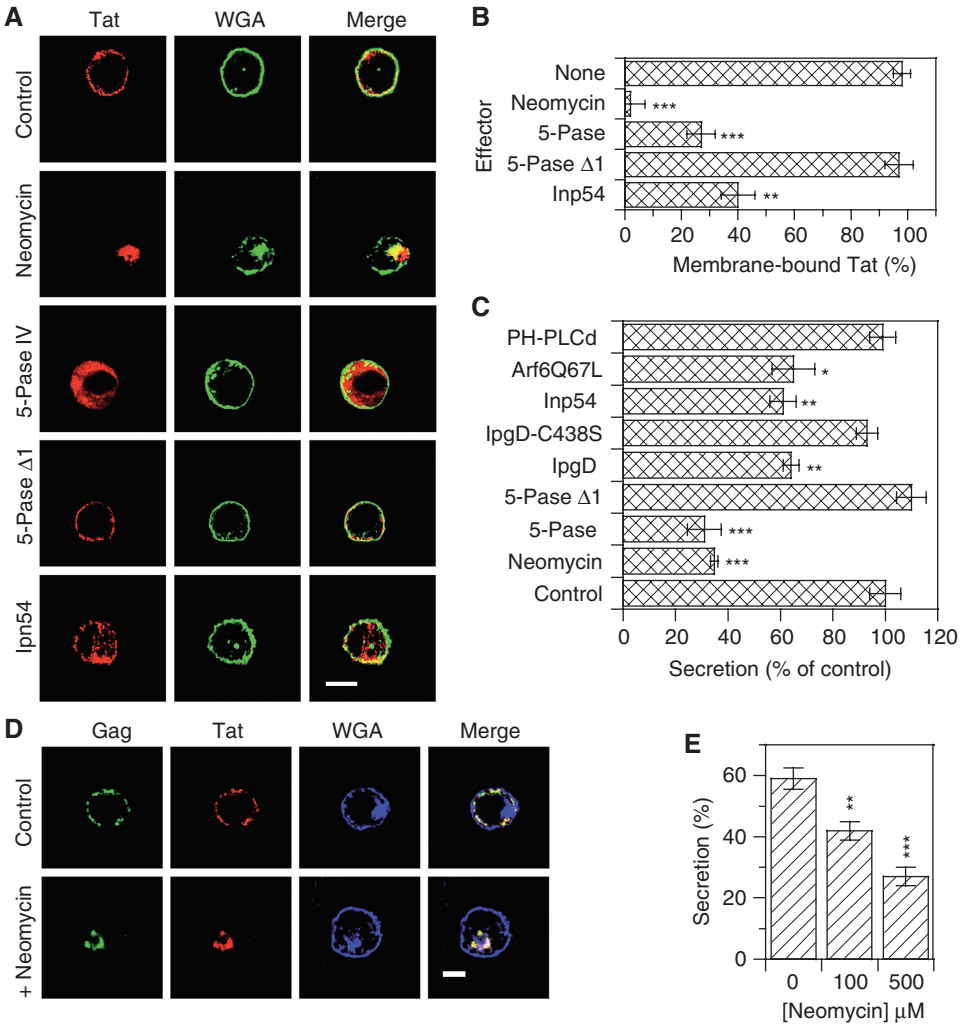

Figure 5 Tat secretion is inhibited when PI(4,5)P_2 is masked, hydrolysed or displaced from the plasma membrane. (**A**) Tat intracellular localization in activated CD4$^+$ primary T-cells. Cells were cotransfected with 1 μg of pBi-Tat and 1 μg of the indicated effector. 5-pase is 5-phosphatase IV and 5-pase Δ1, an inactive mutant. After 1 day, and a 1 h treatment with 2 mM neomycin when indicated, cells were fixed for Tat staining by immunofluorescence. The plasma membrane and the TGN were revealed using WGA. Representative median confocal sections. Bar, 5 μm. (**B**) Quantification of the immunofluorescence results. Images from $n > 20$ cells were recorded and the percentage of cell-fluorescence signal originating from the plasma membrane was determined. (**C**) Tat secretion by Jurkat cells. Tat, luciferase and the indicated effector plasmid were transfected into Jurkat cells before assaying Tat secretion 48 h later. When indicated, 10 mM neomycin was present during the secretion assay. Higher $PH_{PLC\delta}$ doses were not more effective (data not shown). (**D**) Neomycin displaces Tat and Gag from the plasma membrane of infected cells. HIV-1-infected primary T-cells were treated with 2 mM neomycin for 1 h before fixation and localization of Tat and Gag p24 by immunofluorescence combined with WGA staining. Representative median confocal sections; bar, 5 μm. (**E**) Neomycin inhibits Tat secretion by HIV-1-infected primary T-cells in a dose-dependent manner. Cells were incubated in the ELISA plate for 15 h at 37°C in the presence of the indicated concentration of neomycin before processing. The significance of differences with control conditions was assessed using a two-sided Student's *t*-test (***$P < 0.001$; **$P < 0.01$; *$P < 0.02$).

one residue among the three basic residues 49–51 is involved in this interaction. We then performed an Ala scan on the basic residues of the domain to identify important residues. The secretion efficiency of these point mutants was essentially unaffected (Figure 6C). Nevertheless, when the first residues of the domain were progressively replaced by Ala, the secretion efficiency dropped from 82% (R49A) to 58% ((49–50)A) and 1% ((49–51)A). Equivalent mutations on the other end of the domain only weakly affected secretion (70% of secretion for (55–57)A). To monitor and compare the capacity of these mutants to bind PI(4,5)P_2, we used ITC. We found (Figure 6D) that recombinant Tat(49–51)A did not significantly bind PI(4,5)P_2, whereas Tat (55–57)A showed an affinity ($K_d = 42$ nM) similar to that of native Tat ($K_d = 16$ nM). Intracellular localization analysis by immunofluorescence confirmed biochemical data as Tat(55–57)A localized to the plasma membrane of transfected primary CD4$^+$ T-cells, whereas Tat(49–51)A was essentially cytosolic (Figure 6E and F). Similar data were obtained using cell fractionation, except that in that case, Tat(49–51)A was observed in the nuclear and not in the cytosolic fraction (Supplementary Figure S5).

The fact that Tat (55–57)A preserved essentially native PI(4,5)P_2 binding and secretion capacities shows that the loss of these activities by Tat(49–51)A is not merely due to the lack of three positive charges. These combined immunofluorescence, SPR, ITC and secretion data showed that Tat binds PI(4,5)P_2 through residues 49–51 of its basic domain and confirmed that PI(4,5)P_2 binding is a prerequisite for Tat secretion.

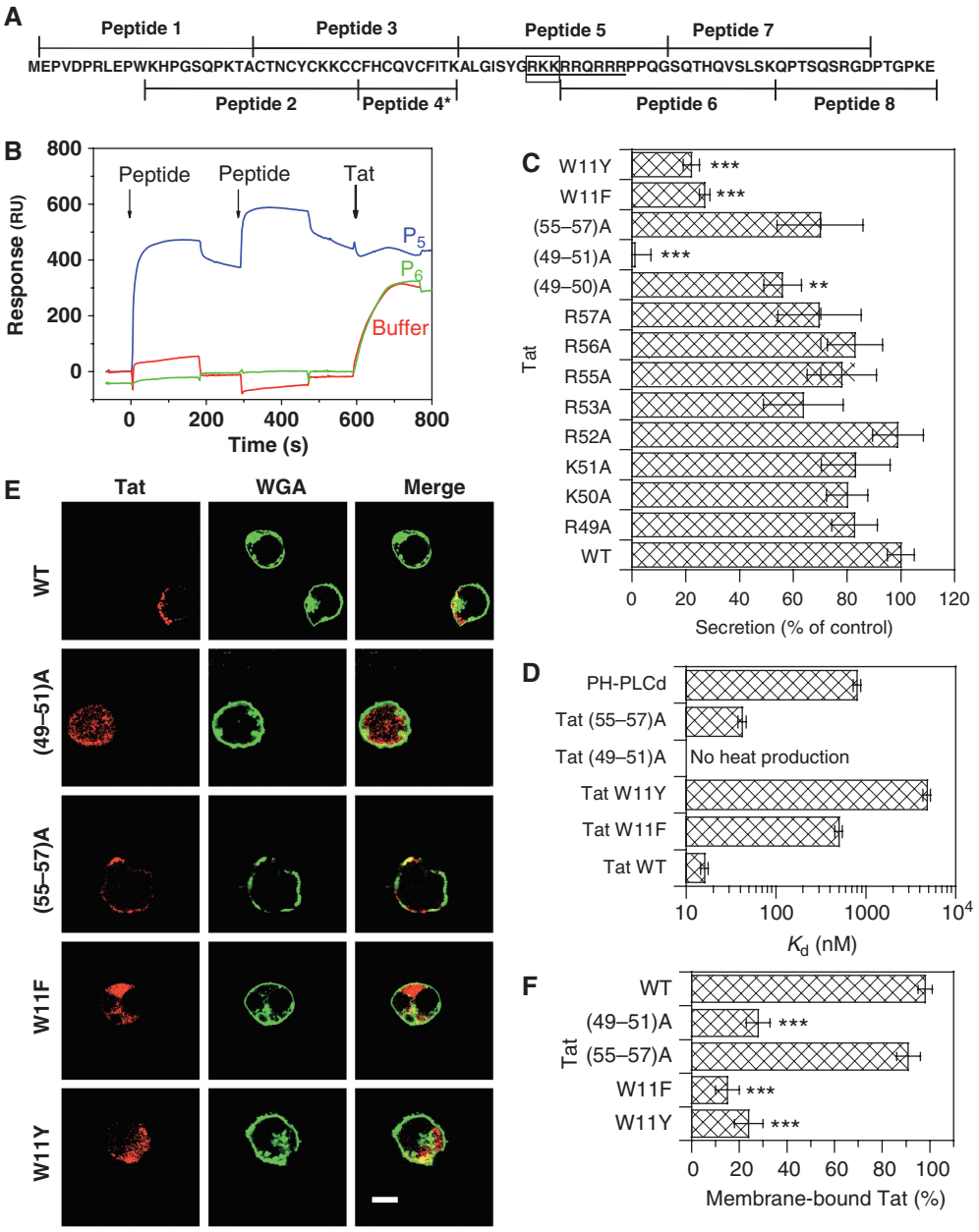

Figure 6 Identification of Tat residues involved in PI(4,5)P_2 binding. (**A**) Sequence of HIV-1 Tat BH10 and of the peptides used for this study. The residues of the basic domain are underlined, and those of the PIP_2-binding site are boxed. Peptide 4* contains twice the indicated sequence. Cys-containing peptides were reduced with 10 mM DTT before use. (**B**) SPR sensorgrams illustrating the inhibition by Tat peptides of Tat binding to PI(4,5)P_2 liposomes. Peptides were injected twice before applying Tat, as indicated by the arrows. The results of peptide 5 (P5) and 6 (P6) are shown. The other peptides behaved as P6 or buffer. The running buffer for SPR was 0.4 M NaCl, 10 mM HEPES, pH 7.4. (**C**) Secretion assays. Jurkat cells were transfected with luciferase and the indicated Tat mutant before assaying Tat secretion by ELISA 48 h later. (**D**) Affinity of Tat mutants and $PH_{PLC\delta}$ for PIP_2 liposomes as measured by ITC. Liposomes were sequentially injected into a microcalorimeter cuvette containing the protein. Heat production was monitored and enabled K_d determination. Tat(49–51)A did not produce any heat and, therefore, did not bind PIP_2. (**E**) Intracellular localization of Tat mutants. Primary $CD4^+$ T-cells were transfected with the indicated Tat mutant; 24 h later, cells were fixed and permeabilized for Tat immunofluorescence combined with WGA staining. Bar, 5 μm. (**F**) Quantification of the immunofluorescence results. Images from $n > 20$ cells were recorded and the percentage of cell-fluorescence signal originating from the plasma membrane was determined. The significance of differences with WT Tat was assessed using a two-sided Student's *t*-test (***$P < 0.001$; **$P < 0.01$).

Tat requires a lipid membrane for insertion on PIP_2 binding

As three positive charges of Tat are involved in the binding of PI(4,5)P_2 that has 3–5 negative charges (McLaughlin *et al*, 2002), the Tat–PI(4,5)P_2 interaction should be stoichiometric. Titration of Tat with PI(4,5)P_2–liposomes by ITC indeed revealed a stoichiometry of one PI(4,5)P_2 per Tat molecule (Table I). Surprisingly, this specificity was lost when using a water-soluble PI(4,5)P_2 analogue, diC8-PI(4,5)P_2, or the PI(4,5)P_2 head group (Ins(1,4,5)P_3) for which a 3–4 ligands/Tat interaction was observed, indicating that these soluble ligands bound to virtually all Tat-positive charges ($n = 17$). In addition, when using liposomes, the ITC injection peaks were followed by a characteristic slow binding event

Table I Titration calorimetry of inositol phosphate binding to Tat and $PH_{PLC\delta}$

	N (Tat:ligand)	K_d (nM)	ΔG (kJ/mol)	ΔH (kJ/mol)	$T\Delta S$ (kJ/mol)
$PH_{PLC\delta}$:PIP_2 liposomes	1:1.0	900	−34.8	−18.7	+16.1
Tat:Ins(1,4,5)P3	1:3.6	24	−42.8	+181.4	+224.2
Tat:PIP_2 liposomes	1:1.0	16	−43.9	+129.2	+173.1

N, stoichiometry; K_d, dissociation constant. Precisions on K_d are ± 10%.
Proteins were present in the cell and PIP_2 liposomes (PC/PG/PI(4,5)P_2 75/20/5) or Ins(1,4,5)P_3 were sequentially injected.

(Figure 7A) that was not observed when using diC8-PI(4,5)P_2 (data not shown), Ins(1,4,5)P_3 (Figure 7B) or for the $PH_{PLC\delta}$–liposome interaction (Figure 7C). These three titration curves (Figure 7A-C) were strikingly different.

Regarding the thermodynamics, PI(4,5)P_2 recognition by PH domains is known to be an enthalpy-driven reaction (Lemmon *et al*, 1995) (Table I), as expected for a binding event involving hydrogen bonding or ionic interactions with phosphate groups. Surprisingly, under the same experimental conditions, Tat interactions with PI(4,5)P_2 liposomes were driven by a very favourable entropy that compensated for a large unfavourable enthalpy (Table I). This unfavourable enthalpy was unexpected, and the association of Tat with PI(4,5)P_2 liposomes clearly seems to be atypical in this respect. We also noted a significant reduction in favourable entropy for Tat titrations with liposomes as compared with those with Ins(1,4,5)P_3 (Table I) or diC8-PI(4,5)P_2 (data not shown). Together with the slow binding event apparent for Tat–liposome interactions (Figure 7A), this could be indicative for Tat folding and/or membrane insertion.

These ITC results thus indicated that Tat requires a membrane to bind PI(4,5)P_2, and suggested that the intrinsically unstructured Tat adopted a 3D-fold on interaction with PI(4,5)P_2–liposomes and directly engaged interactions with the lipid membrane itself. This interpretation was consistent with the observations that Tat did not bind to PI(4,5)P_2 spotted on a blot membrane or coated on an ELISA plate (data not shown). This was directly confirmed by the results of monolayer penetration experiments. In these studies, phospholipid monolayers of a chosen initial surface pressure (π_0) were spread at constant area and the change in surface pressure ($\Delta\pi$) was monitored after protein injection into the subphase. The extrapolation of the $\Delta\pi$ versus π_0 plot yields the critical surface pressure (π_c), which provides a π_0 upper limit of a monolayer that a protein can insert into. The cell surface pressure of biological membranes has been estimated to be 30–35 mN/m (or dyne/cm), and any protein that presents a π_c above this threshold can, therefore, spontaneously penetrate into biological membranes (Stahelin *et al*, 2003). Although Tat did not insert into PC/PG monolayers, in the presence of 5% PI(4,5)P_2, Tat showed exceptionally high membrane penetrating power ($\pi_c \sim 36$ mN/m; Figure 7D), that is higher than that of Epsin ENTH domain ($\pi_c \sim 31$ mN/m; Stahelin *et al*, 2003) for instance. This result indicated that Tat can spontaneously insert into the inner leaflet of the plasma membrane.

Molecular basis for Tat-high affinity for PIP_2

How does Tat insert into membranes on PI(4,5)P_2 binding? According to the poor affinity of the transduction peptide for liposomal PI(4,5)P_2 (Figure 6B), this interaction involves, in addition to the Tat basic domain, the participation of other parts of the molecule. Among hydrophobic residues that could be involved in membrane interaction, Tat owns a single and well-preserved Trp (Supplementary Figure S6; Pantano and Carloni, 2005) that enables Tat insertion into the endosome membrane during endocytosis of extracellular Tat (Yezid *et al*, 2009).

To examine whether Tat Trp indeed inserted into the membrane on Tat binding to PI(4,5)P_2, we monitored the quenching of Tat-Trp fluorescence on binding to liposomes containing the hydrophobic quencher 10-doxylnonadecane (10-DN) (Caputo and London, 2003). Strong Trp-fluorescence quenching was observed when using PC/PS/PI(4,5)P_2/10-DN vesicles, whereas fluorescence was not affected when using vesicles lacking PI(4,5)P_2 (Figure 7E). This result confirmed that Tat inserts into the membrane on PI(4,5)P_2 binding, and showed that Tat Trp is involved in this insertion process. Regarding the kinetics, insertion was essentially complete within 2 min. This is in agreement with the time scale of heat production detected during Tat–liposome interaction (Figure 7A).

We then made two conservative (W11F and W11Y) mutations on Trp11. We first monitored whether these mutations preserved native Tat biological activity, as monitored using the transactivation activity of the protein. This activity indeed requires Tat interaction with several partners (proteins and RNA) that recognize different domains of the protein (Jeang *et al*, 1999). The W11F mutation induced a drop of 50% in transactivation activity. This indicated a conformational problem in this mutant. Tat-W11Y showed native transactivation activity, suggesting that it preserved a normal conformation and reactivity of the molecule (Yezid *et al*, 2009).We then monitored the PIP_2-binding capacity of these mutants by ITC. Replacement of Tat-Trp11 induced a drastic loss in the avidity for PI(4,5)P_2 as Tat-W11F and Tat-W11Y bound PI(4,5)P_2 30- and 300-fold less efficiently than WT Tat, respectively (Figure 6D). Keeping in mind the reservations regarding Tat-W11F conformation, it should be noted that the affinity of Trp11-mutant for PI(4,5)P_2 is consistent with the respective ability of these residues to insert into membranes: Trp > > Phe > Tyr (White and Wimley, 1999).

To confirm the function of Tat-W11 in PI(4,5)P_2 binding and Tat recruitment at the plasma membrane, we examined the intracellular localization of W11 mutants. They were both largely cytosolic (Figure 6E and F). This observation was confirmed by the results of secretion assays, as both W11F and W11Y mutations strongly inhibited Tat secretion by Jurkat cells (by ∼80%; Figure 6C). Collectively, these results showed that Tat Trp11 enables Tat membrane insertion that is strictly required for Tat binding to PI(4,5)P_2, and thus for Tat secretion. This tight link and coupling between membrane

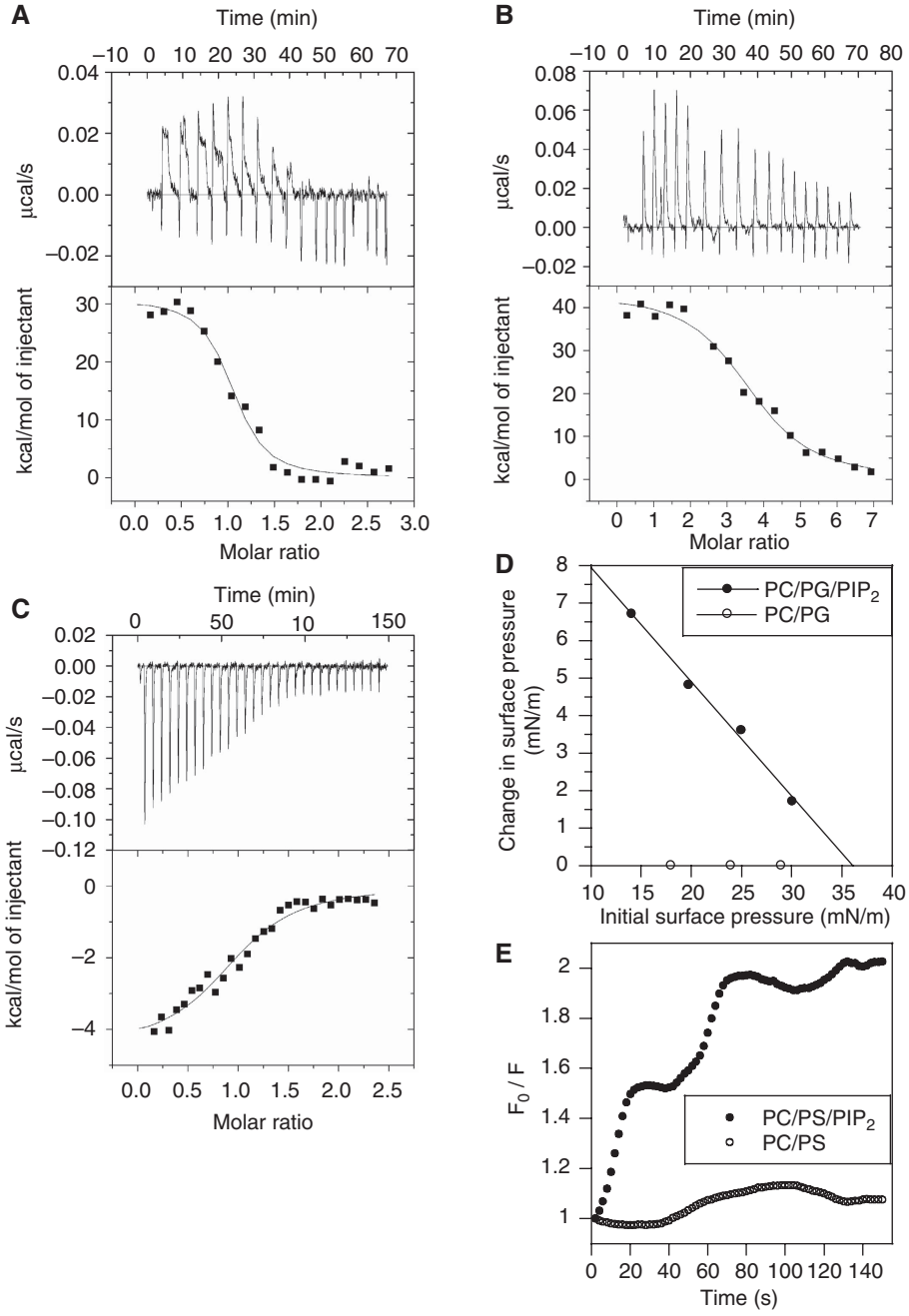

Figure 7 Tat inserts into membranes on PI(4,5)P_2 binding. Raw ITC data of Tat binding to (**A**) PI(4,5)P_2 liposomes (PC/PG/PI(4,5)P_2 75/20/5) and (**B**) Ins(1,4,5)P_3. (**C**) Binding of GST–$PH_{PLC\delta}$ to PI(4,5)P_2 liposomes. Ins(1,4,5)P_3 or PI(4,5)P_2 liposomes were injected into the protein solution and heat production was monitored. The heat resulting from buffer injection was subtracted from the binding curves. Tat binding to diC8-PI(4,5)P_2 showed narrow heat production peaks just as Ins(1,4,5)P_3 (data not shown). (**D**) Tat inserts into phospholipid monolayers. Tat insertion into monolayers was monitored using $\Delta\pi$ as a function of π_0. Monolayers were made of PC/PG (75/25) or PC/PG/PI(4,5)P_2 (75/20/5) as indicated, and the subphase was 150 mM NaCl, 50 mM citrate, pH 7.0. For conversion, 1 mN/m = 1 dyne/cm. Similar data were obtained using PS instead of PG (data not shown). (**E**) 10-DN quenching of Tat Trp fluorescence. Tat (2.5 µM) was quickly mixed with lipid vesicles composed of PC/PS (75/25) or PC/PS/PIP_2 (75/20/5) containing or not 10% of the 10-DN quencher. Trp fluorescence was then recorded every 2 s. F_0/F is the ratio of fluorescence intensity in samples without quencher relative to that with 10-DN (Caputo and London, 2003). The results of a representative experiment that was repeated three times.

penetration and PIP_2 binding is the basis of the Tat requirement for a lipid membrane to bind PI(4,5)P_2.

Secreted Tat is biologically active

It was important to check the biological activity of secreted Tat in our experimental system. To this end, we first used a well-established transcellular transactivation assay (Helland *et al*, 1991; Marcuzzi *et al*, 1992; Ensoli *et al*, 1993). Donor cells were transfected with Tat (WT or W11Y) or EGFP as a control, and recipient cells with luciferase reporter plasmids. Donor and recipient cells were then mixed and collected for luciferase assays after various times of cocultivation. A time-

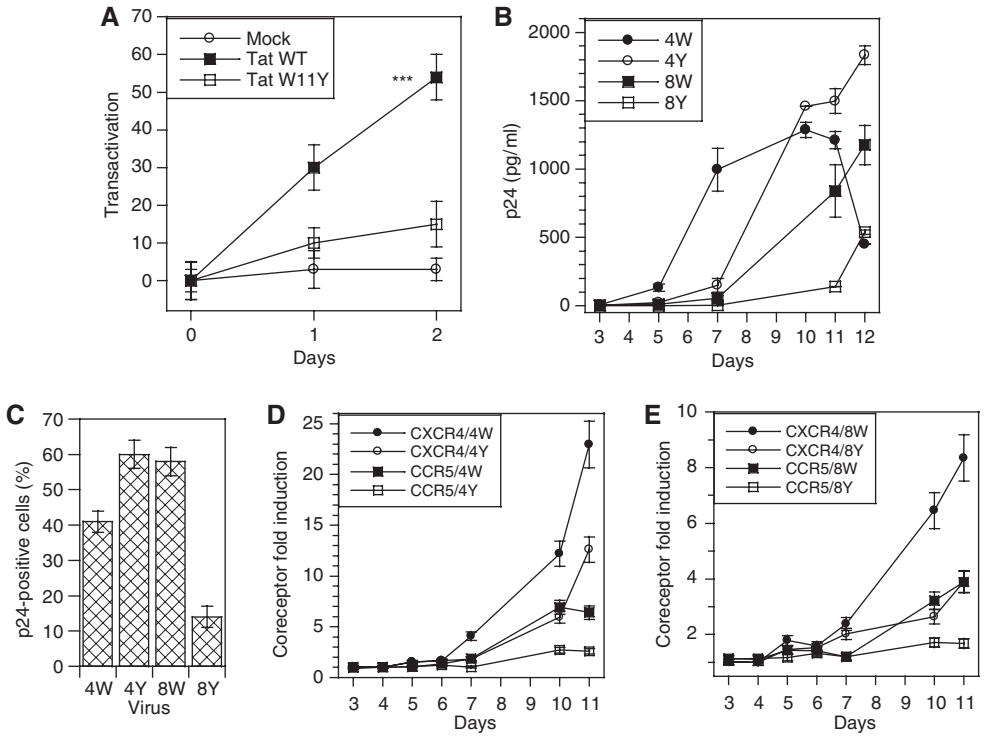

Figure 8 Secreted Tat is biologically active. (**A**) Transcellular transactivation by secreted Tat. Jurkat cells were transfected with WT Tat, Tat-W11Y or EGFP (mock); 18 h after transfection, cells were mixed (1/1) with Jurkats cells transfected with luciferase vectors, one encoding firefly luciferase under the control of HIV-1 LTR, and the other renilla luciferase under the control of a Tat-independent promoter. Cells were harvested for luciferase assays after the indicated coculture time, and transactivation was calculated using the increase in the firefly/renilla activity ratio (%). (**B**, **C**) Secreted Tat differentially affects virus replication according to tropism. Jurkat CD4-CCR5 T-cells that express both CXCR4 and CCR5 were infected with an X4 (pNL4-3) or an R5 (AD8) HIV-1 variant, bearing either WT Tat or Tat-W11Y as indicated by 4W, 4Y, 8W and 8Y. Infection was monitored using (**B**) p24 ELISA of culture supernatants and (**C**) intracellular p24 staining and FACS analysis using quadrant statistics. Data shown are representative of three different experiments. Similar results were obtained using PBMCs as target cells (data not shown). (**D**, **E**) Secreted Tat induces coreceptor expression. Coreceptor expression by Jurkat CD4-CCR5 T-cells infected with X4 (**D**) or R5 (**E**) variants was monitored by FACS analysis. Expression was quantified as the average fluorescence of the cell population, and the fold induction of CXCR4 and CCR5 was obtained by comparison with expression in control samples.

dependent transcellular transactivation was observed in the case of WT-Tat (Figure 8A). Tat-W11Y that is poorly secreted (Figure 6C) and unable to reach the cytosol of target cells (Yezid *et al*, 2009) did not transactivate in this assay, although it showed native transactivation activity when coexpressed with luciferase vectors (Yezid *et al*, 2009), Hence, secreted Tat is capable to enter recipient cells to transactivate, and is thus biologically active.

Secreted Tat strongly affects HIV-1 multiplication

Transcellular transactivation assays are not very sensitive (Ensoli *et al*, 1993), and we thought of using another effect of extracellular Tat to confirm that secreted Tat is active on target cells. Extracellular Tat was found to affect HIV-1 multiplication at the level of virus coreceptors (Huang *et al*, 1998; Weiss *et al*, 1999; Ghezzi *et al*, 2000; Xiao *et al*, 2000). As a Tat mutant that transactivates properly, but is not secreted, was not available, these studies used recombinant Tat and not Tat produced by infected cells. We took advantage of the Tat-W11Y mutant that retains native transactivation activity (Yezid *et al*, 2009), but is unable to cross membranes (Figure 6C; Yezid *et al*, 2009). We prepared recombinant viruses bearing the W11Y mutation either in an X4 or an R5 background, and used these viruses to infect CCR5-transfected Jurkat T-cells or PBMCs. These systems provided similar results. We monitored infection using extracellular- and intracellular-p24 assays and assessed coreceptor expression at the cell surface using FACS analysis. The results of extracellular p24 determinations (Figure 8B for Jurkat CD4-CCR5 cells) showed that all viruses were replicative. Regarding X4 (pNL4-3) viruses, the WT initially replicated more quickly, but a maximum was reached at day 10 and virus production decreased at later times. The highest virus titres were obtained with the mutant (Tat-W11Y) X4 virus (+40% compared with WT). Intracellular p24 assays by FACS (Figure 8C) or western blots (not shown) confirmed that X4-Tat-W11Y replicated more efficiently than the WT X4 viruses. Secreted WT Tat induced very strongly (up to 23-fold) CXCR4 expression (Figure 8D). CCR5 induction was lower (up to six-fold), but this weaker effect could be related to the specific genetic background of Jurkat CD4-CCR5 cells. The mutant (Tat-W11Y) X4 virus was much less efficient in increasing coreceptor levels (up to 12-fold for CXCR4 and three-fold for CCR5) and its effect likely represents the participation of infected cells.

When R5 (AD8) viruses were used, the mutant replicated less actively than the WT (Figure 8B and C). As noticed for X4 viruses, the WT R5 virus was at least two-fold more efficient than the mutant in increasing coreceptor expression (Figure 8E).

Altogether, these results are consistent with established Tat effects on HIV-1 coreceptors. The effect on CXCR4 is the most complex. Extracellular Tat at 2–200 nM is known to bind CXCR4, thereby inhibiting infection by X4 viruses (Ghezzi *et al*, 2000; Xiao *et al*, 2000). Nevertheless, as shown earlier using subnanomolar concentrations of exogenous Tat (Huang *et al*, 1998), Tat strongly induced CXCR4 expression (Figure 8D). As a result of these two opposite and concentration-dependent effects, the WT X4 virus started to multiply more efficiently than the mutant (Figure 8B). This is noticeable at day 7 in which WT X4 had already induced significant CXCR4 expression (Figure 8D). After day 10, when Tat accumulated in the medium, its inhibitory effect on the multiplication of WT X4 became dominant (Figure 8B and C). This concentration-dependent effect of Tat might modulate the spread of X4 viruses in patients by favouring infection in which infected cells are scarce (low Tat concentration) and inhibiting viral production in which infected cells are concentrated (high Tat concentration).

Regarding R5 viruses, our data confirmed those obtained using recombinant Tat and showing that extracellular Tat induced CCR5 (Huang *et al*, 1998; Weiss *et al*, 1999). Therefore, WT R5 viruses that trigger efficient Tat secretion have more CCR5 available for entry than W11Y R5 viruses (Figure 8E) and as a result multiply more quickly (Figure 8B). Secreted Tat thus regulates HIV-1 multiplication at the coreceptor level. For X4 viruses, this effect, positive when infection starts, becomes negative when Tat reach a threshold concentration in the nanomolar range, whereas Tat favours the multiplication of R5 viruses.

Discussion

Although HIV-1-infected cells were found to secrete Tat 19 years ago (Ensoli *et al*, 1990), this process remained poorly characterized (Chang *et al*, 1997). Meanwhile, a lot of studies showed that extracellular Tat was indeed a viral toxin that could affect the biological activity or the life span of different cell types, (Rubartelli *et al*, 1998; Gallo, 1999; Huigen *et al*, 2004). Nevertheless, Tat function was thought to be essentially restricted to the control of viral RNA production (Chiu *et al*, 2002). This general belief was largely due to the observations that transfected Tat was a nuclear or a nucleolar protein in most laboratory T-cell lines such as Jurkats (Figure 2A and B).

Tat intracellular localization

Here, we found that Tat accumulated at the plasma membrane in primary $CD4^+$ T-cells. This was observed in both HIV-1-infected and Tat-transfected cells using immunofluorescence and cell fractionation (Figure 2). Hence, viral infection is not involved in Tat targeting to the plasmalemma in this cell type. As HIV-1 replicates in primary $CD4^+$ T-cells, nuclear accumulation is not required for transactivation. This interpretation is consistent with the subnanomolar affinities involved in the assembly of the cyclin T1–Tat–TAR ternary complex (Zhang *et al*, 2000). As these interactions are at least 20-fold tighter than Tat–PI(4,5)P_2 interaction, and as significant amounts of Tat are bound to PI(4,5)P_2 in the infected cell (Figure 2D and E), all TAR should have bound a Tat molecule. Hence, in primary $CD4^+$ T-cells, Tat transcriptional activity only requires and uses minute Tat amounts, allowing the infected cell to export most of the protein.

This interpretation was confirmed by the results obtained using Jurkat cells transfected with Tat-NES. The NES, when attached to Tat C-terminus, caused its relocalization to the cytosol and the plasma membrane, whereas transactivation activity was only moderately affected (Supplementary Figure S2). Hence, significant transactivation by Tat does not require Tat nuclear/nucleolar accumulation and Tat nuclear-concentration levels required to insure robust transactivation are below the immunofluorescence detection threshold.

Tat secretion is efficient and relies on PI(4,5)P_2 binding

We found that, although unconventional, HIV-1 Tat secretion is an efficient process as 4–5% of cell-associated Tat is exported hourly. Interestingly, the extracellular Tat concentration observed after overnight incubation of infected $CD4^+$ T-cells (5.10^6 cells/ml) reached 0.25 nM, a value that falls within the Tat-concentration range (0.18–3.6 nM) that was observed in the sera of HIV-1-infected patients (Xiao *et al*, 2000). This secretion efficiency also means that during the life span of the infected cell $\sim$2/3 of synthesized Tat will be exported, showing that the outside medium is a major destination for Tat.

Tat secretion relies on PI(4,5)P_2 binding. Such a requirement was recently observed for the unconventional secretion of FGF-2, although compared with Tat, this cytokine showed lower specificity and affinity for PI(4,5)P_2. Moreover, FGF-2 does not require a membrane to bind PI(4,5)P_2 (Temmerman *et al*, 2008). Hence, although these proteins are similarly targeted to the plasma membrane, the mechanisms of PI(4,5)P_2 recognition and membrane translocation are likely different for Tat and FGF-2.

Tat is not the only HIV-1 protein recruited by PI(4,5)P_2 at the plasma membrane. This is also the case for Gag (Ono *et al*, 2004) and both proteins were indeed found to colocalize at the infected-cell plasmalemma (Figure 2D and E) and on peri-Golgi structures when they were displaced from PI(4,5)P_2 by neomycin (Figure 5D). As HIV-1 virions were found to be enriched in this phosphoinositide (Chan *et al*, 2008), this raises the possibility that Tat could be included into virions, as discussed earlier (Chertova *et al*, 2006).

Molecular bases for Tat–PI(4,5)P_2 high affinity

The bases for Tat–PI(4,5)P_2 interaction are original in several respects. It was first surprising to find that, although the Tat basic domain contains eight basic residues out of a total of nine, only the first three were involved in PI(4,5)P_2 recognition. This indicates that Tat, although refractory to crystallization and for which no precise 3D structure is currently available, nevertheless undergoes some kind of molecular organization, at least on ligand docking. This interpretation was confirmed by ITC data showing that liposomal PI(4,5)P_2 induced Tat conformational modifications (Figure 7A).

The sequence of molecular remodelling triggered by PI(4,5)P_2 binding and culminating with Tat membrane insertion and translocation remains to be identified. Nevertheless, as Tat Trp is buried within resting Tat (Bayer *et al*, 1995), whereas PI(4,5)P_2 binding generated structural modifications that could be detected by ITC (Figure 7A), it seems likely that interaction with PI(4,5)P_2 precedes and triggers Trp exposure.

Tat is an original PI(4,5)P_2 ligand because of its high affinity and its strict requirement for a membrane to bind this lipid. These two specificities have the same molecular basis, Tat single Trp residue that inserts into membranes on PI(4,5)P_2 binding, stabilizes the interaction and allows Tat secretion. These events are thus governed by residues 11 and 49–51 of Tat. Interestingly, despite HIV-1 high mutation rate (Walker and Burton, 2008), among the most conserved Tat residues from different viral isolates, residues 11 and 49–51 were indeed present, but not 55–57 (Supplementary Figure S6; Pantano and Carloni, 2005).

The high affinity of Tat for PI(4,5)P_2 indicates that the function of this interaction is unlikely restricted to Tat secretion. Indeed, overexpression of $PH_{PLC\delta}$ prevents the PI(4,5)P_2-mediated recruitment at the plasma membrane of cell machineries that enable clathrin-mediated endocytosis (Jost *et al*, 1998), phagocytosis (Botelho *et al*, 2000) or exocytosis (Holz *et al*, 2000) and inhibits these processes. As Tat has a 50-fold better affinity for PI(4,5)P_2 than $PH_{PLC\delta}$ (Table I) and can accordingly displace it from the cell membrane (Figure 4), it could, therefore, be reasonably concluded that Tat, even at minute concentrations, would produce similar or more pronounced effects on these cell activities, which are crucial for proper immune system function. As Tat is exported and can enter uninfected cells (Vendeville *et al*, 2004), this original and intriguing capacity of Tat to perturb PI(4,5)P_2-mediated protein recruitment could be involved in immune system dysfunction during AIDS.

Conclusion

The main question raised by our study is why does HIV-1 trigger massive Tat export? The answer probably lies in the vast body of literature that described the pronounced effects of extracellular Tat on a variety of cell types (Rubartelli *et al*, 1998; Gallo, 1999; Huigen *et al*, 2004). The preservation among Tats of important residues involved in Tat secretion indeed indicates that the paracrine activity of Tat is critical for HIV-1 multiplication and could be an interesting target to develop future anti-HIV-1 therapeutics.

Materials and methods

Expression vectors

Tat mutants were generated from pBi-Tat or Pet11d-Tat (BH10 isolate, 86 residues) using Quickchange kits (Stratagene). Coding sequences were entirely sequenced (Cogenics, Meylan, France). Recombinant Tat or Tat mutants were purified from *Escherichia coli* as described (Vendeville *et al*, 2004). Expression vectors coding for $PH_{PLC\delta}$-EGFP and its inactive mutant (R40L) were kindly provided by Tamas Balla (NICHD, Bethesda); PTEN and its G129E mutant by Patrick Raynal (INSERM, Toulouse, France); 5-phosphatase IV and its Δ1 mutant by Akira Ono (NCI, Frederick); Arf6-Q67L by Julie Donaldson (NIH, Bethesda); IpgD, IpgD-C438S and Inp54 by Bernard Payrastre (INSERM, Toulouse); PH_{Akt}-EGFP and GAB1-EGFP by Georges Bismuth (Institut Cochin, Paris, France) and GST–$PH_{PLC\delta}$ by Alexander Gray (University of Dundee, UK).

Cells

Primary $CD4^+$ T-cells were purified from human blood by density gradient centrifugation (Ficoll Hypaque) and immunomagnetic-positive selection (Dynal). The human $CD4^+$ T-cell line Jurkat E6.1 was from the American Type Culture Collection. Cells were transfected using electroporation or infected by HIV-1 as indicated. Cell fractionation was performed using a subcellular protein fractionation kit (Thermo Scientific). Details are provided in Supplementary Data.

Secretion assays

Jurkat cells were electroporated (Vendeville *et al*, 2004) with pBi-Tat (20 μg), pBi-firefly luciferase (2 μg), pUHD (2 μg; required for expression from pBi vector) and effector plasmid (10 μg) when indicated. Two days after transfection, cells were washed and resuspended in medium prepared from degassed RPMI, 10% FCS and freshly diluted 20 μM 2-mercaptoethanol. They were then transferred (7.5×10^5 cells/well, in triplicate) to an ELISA FluoroNunc plate that had been coated overnight at 4°C with monoclonal anti-Tat antibody (1 μg/ml in 50 mM sodium carbonate pH 9.6) before saturation with 8% (w/v) skimmed milk in phosphate-buffered saline (PBS). Dilutions of recombinant Tat (19 pg—1.25 ng/well) were also added to the plate for calibration purposes. After 6 h at 37°C (except when otherwise stated), cells were transferred to microtubes, centrifuged and the supernatant was frozen for later luciferase assay. Cells were resuspended in passive lysis buffer prepared from degassed water. Part of the lysate was then used directly to assay intracellular Tat by ELISA using a fresh plate prepared as described above (including Tat standards), whereas the rest was frozen for the luciferase assay that was performed using a Promega kit. The end of the ELISA procedure involved washes with PBS then with PBS/0.05% Tween, incubation with rabbit anti-Tat antibodies for 1 h, washes with PBS/Tween, 1 h with peroxidase-labelled goat anti-rabbit antibodies, washes with PBS/Tween and revelation using 3,3,5,5-tetramethylbenzidine. Secretion was calculated using the Tat amounts present in the medium and intracellularly using the medium/(intracellular + medium) formula. The same protocol was used for infected cells. They were collected 3 days after infection (p24 from 48 to 88 ng/ml), before plating 10^6 cells/well of the ELISA plate and overnight incubation (12–18 h). HIV-1 p24 and Nef secretion were quantified using commercial sandwich ELISA kits (Ingen, France and ImmunoDiagnostics Inc., respectively).

Immunofluorescence

T-cells were allowed to adhere to alcian-blue-coated coverslips for 3 min at room temperature and were fixed in 3.7% paraformaldehyde before permeabilization with 0.1% saponin. Tat, Ki67 or Histone H1 were then revealed by indirect immunofluorescence (Vendeville *et al*, 2004). WGA-Cy5 was used to label glycoproteins on the plasma membrane and in the TGN. For quantification of Tat or $PH_{PLC\delta}$ displacement from the plasma membrane, the ImageQuant software was used. Two circles (or more elaborated forms) were drawn on the cell-fluorescence image, one just outside the cell and one just beneath the membrane. The fluorescence signal present in the circles was then used to calculate the proportion of cell labelling coming from the cytosol and the plasma membrane. A minimum of 30 cells were scored for each condition.

Transcellular transactivation assays

Jurkat cells were transfected (Vendeville *et al*, 2004) with 10 μg of a vector expressing WT Tat, Tat-W11Y or EGFP; 18 h after transfection, cells were mixed (1/1) with Jurkats cells transfected with 7 μg of pGL3-LTR, which expresses firefly luciferase under control of the Tat-activated HIV-1-LTR promoter, and 1 μg of pRL-TK (Promega) that codes for renilla luciferase under the control of the herpes simplex virus thymidine kinase promoter. Cells were harvested for dual luciferase assays (Promega) after the indicated coculture time, and transactivation was calculated using the increase in the firefly/renilla activity ratio (%) (Vendeville *et al*, 2004).

Lipid techniques

Liposome sedimentation assays were performed as described (Barret *et al*, 2000). Small unilamellar vesicles (Méré *et al*, 2005) were used for SPR (Zimmermann *et al*, 2002) and ITC (Lemmon *et al*, 1995) analysis. Fluorescence and monolayer experiments were performed as detailed (Stahelin *et al*, 2003; Méré *et al*, 2005). Details are provided in Supplementary Data.

Supplementary data

Supplementary data are available at *The EMBO Journal* Online (http://www.embojournal.org).

Acknowledgements

We thank all the people who, directly or indirectly, provided valuable material for this study. We are indebted to the AIDS Research and Reference Reagent Program, NIH, USA and the Programme EVA Centre for AIDS Reagents, NIBSC, UK for reagents. We are also grateful to Nicole Lautredou (IURC Montpellier RIO Imaging) for assistance with confocal analysis, to David Perrais, Laurent Chaloin and David Fenard for help in preliminary experiments, to Laurent Chiche for Tat sequence comparative analysis and to Catherine Lévèque for English editing. This work was supported by grants from the ANRS and Sidaction.

Conflict of interest

The authors declare that they have no conflict of interest.

References

Aharonovitz O, Zaun HC, Balla T, York JD, Orlowski J, Grinstein S (2000) Intracellular pH regulation by Na(+)/H(+) exchange requires phosphatidylinositol 4,5-bisphosphate. *J Cell Biol* **150:** 213–224

Astoul E, Edmunds C, Cantrell DA, Ward SG (2001) PI 3-K and T-cell activation: limitations of T-leukemic cell lines as signaling models. *Trends Immunol* **22:** 490–496

Barret C, Roy C, Montcourrier P, Mangeat P, Niggli V (2000) Mutagenesis of the phosphatidylinositol 4,5-bisphosphate (PIP(2)) binding site in the NH(2)-terminal domain of ezrin correlates with its altered cellular distribution. *J Cell Biol* **151:** 1067–1080

Bayer P, Kraft M, Ejchart A, Westendorp M, Frank R, Rosch P (1995) Structural studies of HIV-1 Tat protein. *J Mol Biol* **247:** 529–535

Blin G, Margeat E, Carvalho K, Royer CA, Roy C, Picart C (2008) Quantitative analysis of the binding of ezrin to large unilamellar vesicles containing phosphatidylinositol(4,5)-bisphosphate. *Biophys J* **94:** 1021–1033

Botelho RJ, Teruel M, Dierckman R, Anderson R, Wells A, York JD, Meyer T, Grinstein S (2000) Localized biphasic changes in phosphatidylinositol-4,5-bisphosphate at sites of phagocytosis. *J Cell Biol* **151:** 1353–1368

Brown FD, Rozelle AL, Yin HL, Balla T, Donaldson JG (2001) Phosphatidylinositol 4,5-bisphosphate and Arf6-regulated membrane traffic. *J Cell Biol* **154:** 1007–1017

Caputo GA, London E (2003) Using a novel dual fluorescence quenching assay for measurement of tryptophan depth within lipid bilayers to determine hydrophobic alpha-helix locations within membranes. *Biochemistry* **42:** 3265–3274

Chan R, Uchil PD, Jin J, Shui G, Ott DE, Mothes W, Wenk MR (2008) Retroviruses human immunodeficiency virus and murine leukemia virus are enriched in phosphoinositides. *J Virol* **82:** 11228–11238

Chang HC, Samaniego F, Nair BC, Buonaguro L, Ensoli B (1997) HIV-1 Tat protein exits from cells via a leaderless secretory pathway and binds to extracellular matrix-associated heparan sulfate proteoglycans through its basic region. *AIDS* **11:** 1421–1431

Chertova E, Chertov O, Coren LV, Roser JD, Trubey CM, Bess Jr JW, Sowder II RC, Barsov E, Hood BL, Fisher RJ, Nagashima K, Conrads TP, Veenstra TD, Lifson JD, Ott DE (2006) Proteomic and biochemical analysis of purified human immunodeficiency virus type 1 produced from infected monocyte-derived macrophages. *J Virol* **80:** 9039–9052

Chiu YL, Ho CK, Saha N, Schwer B, Shuman S, Rana TM (2002) Tat stimulates cotranscriptional capping of HIV mRNA. *Mol Cell* **10:** 585–597

Corbin JA, Dirkx RA, Falke JJ (2004) GRP1 pleckstrin homology domain: activation parameters and novel search mechanism for rare target lipid. *Biochemistry* **43:** 16161–16173

De Matteis MA, Godi A (2004) PI-loting membrane traffic. *Nat Cell Biol* **6:** 487–492

Di Paolo G, De Camilli P (2006) Phosphoinositides in cell regulation and membrane dynamics. *Nature* **443:** 651–657

Dupont E, Prochiantz A, Joliot A (2007) Identification of a signal peptide for unconventional secretion. *J Biol Chem* **282:** 8994–9000

Ensoli B, Barillari G, Salahuddin SZ, Gallo RC, Wong-Staal F (1990) Tat protein of HIV-1 stimulates growth of cells derived from Kaposi's sarcoma lesions of AIDS patients. *Nature* **345:** 84–86

Ensoli B, Buonaguro L, Barillari G, Fiorelli V, Gendelman R, Morgan RA, Wingfield P, Gallo RC (1993) Release, uptake, and effects of extracellular human immunodeficiency virus type 1 Tat protein on cell growth and viral transactivation. *J Virol* **67:** 277–287

Gallo RC (1999) Tat as one key to HIV-induced immune pathogenesis and Tat toxoid as an important component of a vaccine. *Proc Natl Acad Sci USA* **96:** 8324–8326

Ghezzi S, Noonan DM, Aluigi MG, Vallanti G, Cota M, Benelli R, Morini M, Reeves JD, Vicenzi E, Poli G, Albini A (2000) Inhibition of CXCR4-dependent HIV-1 infection by extracellular HIV-1 Tat. *Biochem Biophys Res Commun* **270:** 992–996

Helland DE, Welles JL, Caputo A, Haseltine WA (1991) Transcellular transactivation by the human immunodeficiency virus type 1 tat protein. *J Virol* **65:** 4547–4549

Heo WD, Inoue T, Park WS, Kim ML, Park BO, Wandless TJ, Meyer T (2006) PI(3,4,5)P3 and PI(4,5)P2 lipids target proteins with polybasic clusters to the plasma membrane. *Science* **314:** 1458–1461

Holz RW, Hlubek MD, Sorensen SD, Fisher SK, Balla T, Ozaki S, Prestwich GD, Stuenkel EL, Bittner MA (2000) A pleckstrin homology domain specific for phosphatidylinositol 4, 5-bisphosphate (PtdIns-4,5-P2) and fused to green fluorescent protein identifies plasma membrane PtdIns-4,5-P2 as being important in exocytosis. *J Biol Chem* **275:** 17878–17885

Honing S, Ricotta D, Krauss M, Spate K, Spolaore B, Motley A, Robinson M, Robinson C, Haucke V, Owen DJ (2005) Phosphatidylinositol-(4,5)-bisphosphate regulates sorting signal recognition by the clathrin-associated adaptor complex AP2. *Mol Cell* **18:** 519–531

Huang L, Bosch I, Hofmann W, Sodroski J, Pardee AB (1998) Tat protein induces human immunodeficiency virus type 1 (HIV-1) coreceptors and promotes infection with both macrophage-tropic and T-lymphotropic HIV-1 strains. *J Virol* **72:** 8952–8960

Huigen MC, Kamp W, Nottet HS (2004) Multiple effects of HIV-1 trans-activator protein on the pathogenesis of HIV-1 infection. *Eur J Clin Invest* **34:** 57–66

Jeang KT, Xiao H, Rich EA (1999) Multifaceted activities of the HIV-1 transactivator of transcription, Tat. *J Biol Chem* **274:** 28837–28840

Joliot A, Prochiantz A (2004) Transduction peptides: from technology to physiology. *Nat Cell Biol* **6:** 189–196

Jost M, Simpson F, Kavran JM, Lemmon MA, Schmid SL (1998) Phosphatidylinositol-4,5-bisphosphate is required for endocytic coated vesicle formation. *Curr Biol* **8:** 1399–1402

Keller M, Ruegg A, Werner S, Beer HD (2008) Active caspase-1 is a regulator of unconventional protein secretion. *Cell* **132:** 818–831

Lemmon MA (2003) Phosphoinositide recognition domains. *Traffic* **4:** 201–213

Lemmon MA, Ferguson KM, O'Brien R, Sigler PB, Schlessinger J (1995) Specific and high-affinity binding of inositol phosphates to an isolated pleckstrin homology domain. *Proc Natl Acad Sci USA* **92:** 10472–10476

Marasco WA, Szilvay AM, Kalland KH, Helland DG, Reyes HM, Walter RJ (1994) Spatial association of HIV-1 tat protein and the nucleolar transport protein B23 in stably transfected Jurkat T-cells. *Arch Virol* **139:** 133–154

Marcello A, Cinelli RA, Ferrari A, Signorelli A, Tyagi M, Pellegrini V, Beltram F, Giacca M (2001) Visualization of *in vivo* direct interaction between HIV-1 TAT and human cyclin T1 in specific subcellular compartments by fluorescence resonance energy transfer. *J Biol Chem* **276:** 39220–39225

Marcuzzi A, Weinberger J, Weinberger OK (1992) Transcellular activation of the human immunodeficiency virus type 1 long terminal repeat in cocultured lymphocytes. *J Virol* **66:** 4228–4232

Maroun CR, Naujokas MA, Park M (2003) Membrane targeting of Grb2-associated binder-1 (Gab1) scaffolding protein through Src myristoylation sequence substitutes for Gab1 pleckstrin

homology domain and switches an epidermal growth factor response to an invasive morphogenic program. *Mol Biol Cell* **14:** 1691–1708

McLaughlin S, Wang J, Gambhir A, Murray D (2002) PIP(2) and proteins: interactions, organization, and information flow. *Annu Rev Biophys Biomol Struct* **31:** 151–175

Méré J, Morlon-Guyot J, Bonhoure A, Chiche L, Beaumelle B (2005) Acid-triggered membrane insertion of pseudomonas exotoxin A involves an original mechanism based on pH-regulated tryptophan exposure. *J Biol Chem* **280:** 21194–21201

Nickel W, Rabouille C (2009) Mechanisms of regulated unconventional protein secretion. *Nat Rev Mol Cell Biol* **10:** 148–155

Ono A, Ablan SD, Lockett SJ, Nagashima K, Freed EO (2004) Phosphatidylinositol (4,5) bisphosphate regulates HIV-1 Gag targeting to the plasma membrane. *Proc Natl Acad Sci USA* **101:** 14889–14894

Pantano S, Carloni P (2005) Comparative analysis of HIV-1 Tat variants. *Proteins* **58:** 638–643

Pendaries C, Tronchere H, Arbibe L, Mounier J, Gozani O, Cantley L, Fry MJ, Gaits-Iacovoni F, Sansonetti PJ, Payrastre B (2006) PtdIns5P activates the host cell PI3-kinase/Akt pathway during Shigella flexneri infection. *EMBO J* **25:** 1024–1034

Perelson AS, Neumann AU, Markowitz M, Leonard JM, Ho DD (1996) HIV-1 dynamics *in vivo*: virion clearance rate, infected cell life span, and viral generation time. *Science* **271:** 1582–1586

Ranki A, Lagerstedt A, Ovod V, Aavik E, Krohn KJ (1994) Expression kinetics and subcellular localization of HIV-1 regulatory proteins Nef, Tat and Rev in acutely and chronically infected lymphoid cell lines. *Arch Virol* **139:** 365–378

Rubartelli A, Poggi A, Sitia R, Zocchi MR (1998) HIV-I Tat: a polypeptide for all seasons. *Immunol Today* **19:** 543–545

Sivakumaran H, van der Horst A, Fulcher AJ, Apolloni A, Lin MH, Jans DA, Harrich D (2009) Arginine methylation increases the stability of human immunodeficiency virus type 1 Tat. *J Virol* **83:** 11694–11703

Stahelin RV, Long F, Peter BJ, Murray D, De Camilli P, McMahon HT, Cho W (2003) Contrasting membrane interaction mechanisms of AP180 N-terminal homology (ANTH) and epsin N-terminal homology (ENTH) domains. *J Biol Chem* **278:** 28993–28999

Stauber RH, Pavlakis GN (1998) Intracellular trafficking and interactions of the HIV-1 Tat protein. *Virology* **252:** 126–136

Stebbing J, Gazzard B, Douek DC (2004) Where does HIV live? *N Engl J Med* **350:** 1872–1880

Stephens L, Anderson K, Stokoe D, Erdjument-Bromage H, Painter GF, Holmes AB, Gaffney PR, Reese CB, McCormick F, Tempst P, Coadwell J, Hawkins PT (1998) Protein kinase B kinases that mediate phosphatidylinositol 3,4,5-trisphosphate-dependent activation of protein kinase B. *Science* **279:** 710–714

Temmerman K, Ebert AD, Muller HM, Sinning I, Tews I, Nickel W (2008) A direct role for phosphatidylinositol-4,5-bisphosphate in unconventional secretion of fibroblast growth factor 2. *Traffic* **9:** 1204–1217

Truant R, Cullen BR (1999) The arginine-rich domains present in human immunodeficiency virus type 1 Tat and Rev function as direct importin beta-dependent nuclear localization signals. *Mol Cell Biol* **19:** 1210–1217

Varnai P, Balla T (1998) Visualization of phosphoinositides that bind pleckstrin homology domains: calcium- and agonist-induced dynamic changes and relationship to myo-[3H]inositol-labeled phosphoinositide pools. *J Cell Biol* **143:** 501–510

Vendeville A, Rayne F, Bonhoure A, Bettache N, Montcourrier P, Beaumelle B (2004) HIV-1 Tat enters T-cells using coated pits before translocating from acidified endosomes and eliciting biological responses. *Mol Biol Cell* **15:** 2347–2360

Walker BD, Burton DR (2008) Toward an AIDS vaccine. *Science* **320:** 760–764

Watt SA, Kular G, Fleming IN, Downes CP, Lucocq JM (2002) Subcellular localization of phosphatidylinositol 4,5-bisphosphate using the pleckstrin homology domain of phospholipase C delta1. *Biochem J* **363:** 657–666

Weiss JM, Nath A, Major EO, Berman JW (1999) HIV-1 Tat induces monocyte chemoattractant protein-1-mediated monocyte transmigration across a model of the human blood-brain barrier and up-regulates CCR5 expression on human monocytes. *J Immunol* **163:** 2953–2959

White SH, Wimley WC (1999) Membrane protein folding and stability: physical principles. *Annu Rev Biophys Biomol Struct* **28:** 319–365

Xiao H, Neuveut C, Tiffany HL, Benkirane M, Rich EA, Murphy PM, Jeang KT (2000) Selective CXCR4 antagonism by tat: implications for *in vivo* expansion of coreceptor use by HIV-1. *Proc Natl Acad Sci USA* **97:** 11466–11471

Yezid H, Konate K, Debaisieux S, Bonhoure A, Beaumelle B (2009) Mechanism for HIV-1 TAT insertion into the endosome membrane. *J Biol Chem* **284:** 22736–22746

Zhang J, Tamilarasu N, Hwang S, Garber ME, Huq I, Jones KA, Rana TM (2000) HIV-1 TAR RNA enhances the interaction between Tat cyclin T1. *J Biol Chem* **275:** 34314–34319

Zimmermann P, Meerschaert K, Reekmans G, Leenaerts I, Small JV, Vandekerckhove J, David G, Gettemans J (2002) PIP(2)-PDZ domain binding controls the association of syntenin with the plasma membrane. *Mol Cell* **9:** 1215–1225

